

→ ATMOS 2015

Advances in Atmospheric Science and Applications

HCOOH distributions from IASI with updated retrieval parameters: comparison with ground-based FTIR measurements and IMAGESv2 model

Pommier^{1,*}, M., Clerboux^{1,2}, C., Clarisse², L., Coheur², P.-F., Mahieu³, E., Müller⁴, J.-F., Paton-Walsh⁵ C., Stavrakou⁴, T., Vigouroux⁴, C.

1 Sorbonne Université, CNRS/INSU, LATMOS-IPSL, France - **2** Université Libre de Bruxelles, Belgium - **3** Université de Liège, Belgium - **4** Belgian Institute for Space Aeronomy, Belgium - **5** University of Wollongong, Australia

* Now at Norwegian Meteorological Institute, Norway

matthieup@met.no

8–12 June 2015 | University of Crete | Heraklion, Greece

Tropospheric formic acid (HCOOH)



- HCOOH is **one among the most abundant volatile organic compounds (VOCs)** present in the atmosphere.

- With acetic acid it is a major **contributor to the acidity of precipitation**

- **Many sources:**

secondary product from other organic precursors + small direct emissions by vegetation, ants, biomass burning, soils, agriculture, motor vehicles.

- **Sinks:**

mainly removed through **wet and dry deposition** + (lesser extent) oxidation by the OH radical

HCOOH = short-lived species

lifetime is conditioned by the ratio of precipitation: in the boundary layer 2 days (rainy period) → 6 days (the dry season). **Global lifetime in the troposphere=3–4 days**

Photochemical loss is relatively slow ($\tau \sim 25$ days), so that any HCOOH formed or vented outside of the boundary layer **can be transported for long distances in the free troposphere.**

Recent studies highlight:

A misrepresentation of emission from tropical and boreal forest in models (Stavrakou et al., Nature 2011)

A possible source of HCOOH over the Arctic Ocean (Jones et al., Atmos. Env 2014).

One or more large missing sources (Millet et al., ACPD 2015) → suggest a gap in our current understanding of hydrocarbon oxidation or the existence of an unknown direct flux

 Space missions allow getting global observations of the atmosphere

 Their spatial coverage allows observing remote regions which are sparsely studied by field campaigns

 Limited vertical sensitivity

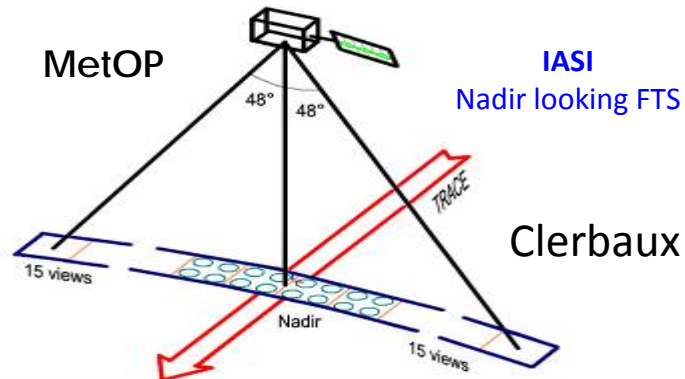
few satellites provide tropospheric HCOOH observations

nadir-viewing instruments: Infrared Atmospheric Sounding Interferometer (**IASI**) (e.g. Coheur et al., 2009), Tropospheric Emission Spectrometer (**TES**) (e.g. Cady-Pereira et al., 2014)

solar-occultation instrument: Atmospheric Chemistry Experiment (**ACE**) (e.g. González Abad, 2009)

limb instrument: Michelson Interferometer for Passive Atmospheric Sounding (**MIPAS**) → global distribution of HCOOH at 10 km (Grutter et al., 2010).

HCOOH: observations with IASI



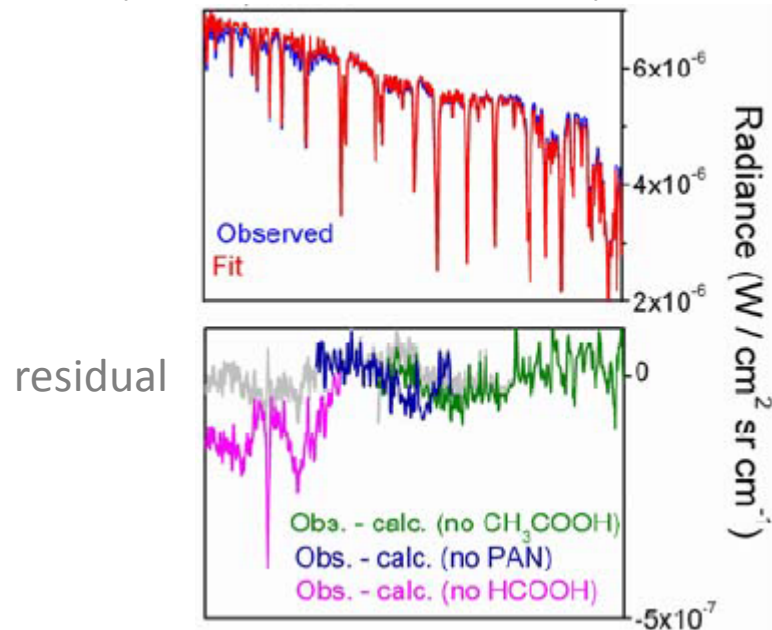
Clerbaux et al. (2009)

- 4 pixels (12 km at nadir)
- 120 spectra along the swath ($\pm 48.3^\circ$ Scan \rightarrow 2400 km), each 50 km along the trace

Small ground pixel size

Global coverage twice daily (morning and evening orbits) – 14 revolutions/day

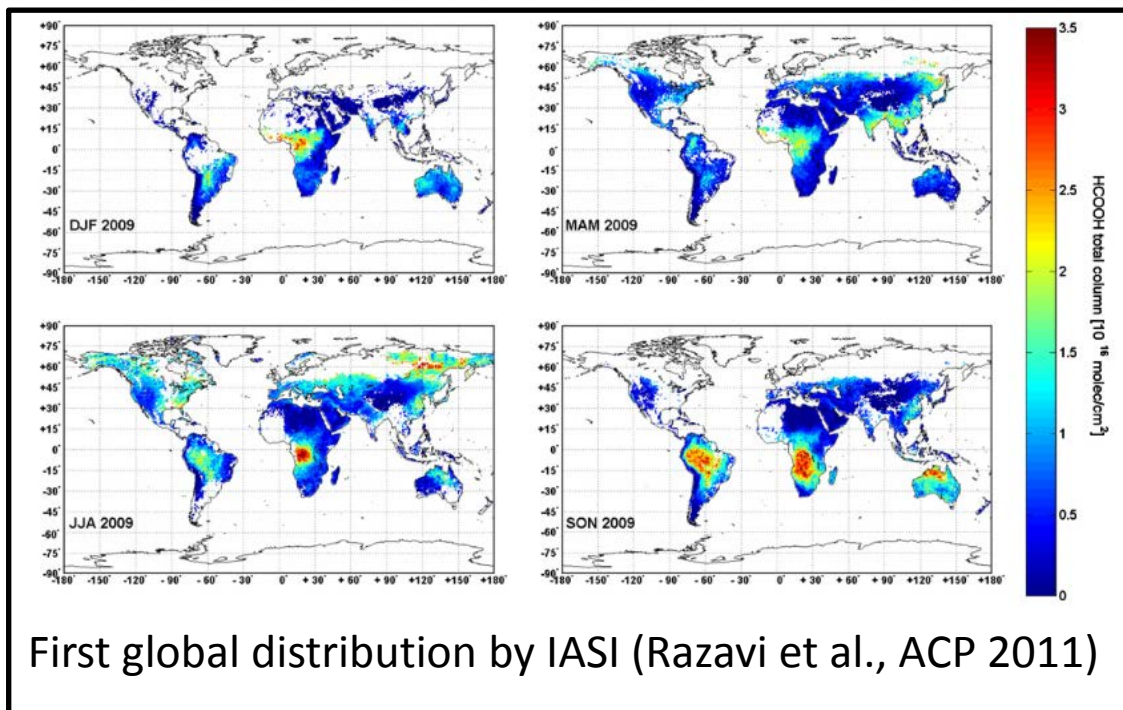
MetOp: First European **meteorological** platform in **polar orbit** launched by EUMETSAT in 2006 (IASI-B launched in 2012)



Coheur et al. (2009)

Spectra given in radiance or brightness temperature
 \rightarrow signal from HCOOH expressed in ΔBT

HCOOH: observations with IASI

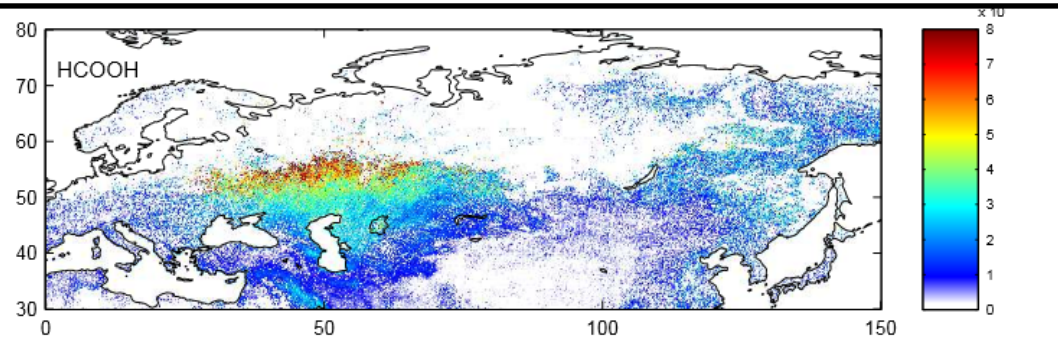


First global distribution by IASI (Razavi et al., ACP 2011)

Objective = find an accurate and fast technique to convert the ΔBT to total columns, avoiding a large computing time
→ necessary to analyze 7 years of data

Detection of extreme events: forest fires in Russia on 2010 (R'Honi et al., ACP 2013)

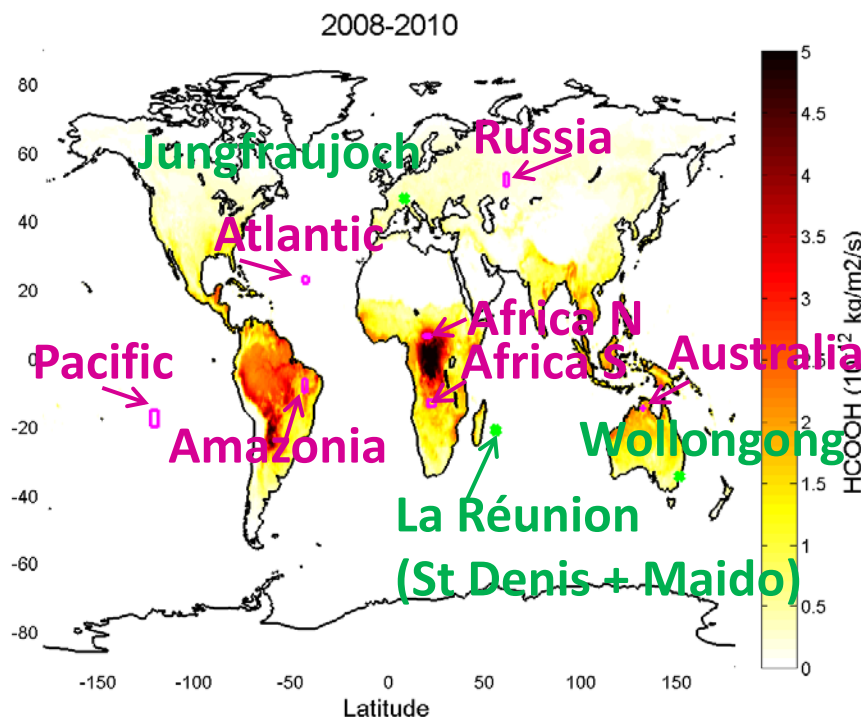
Retrieval relevant for huge amount of HCOOH



HCOOH: Retrieval approach (1/2)

MEGAN-MACC HCOOH emissions for the period between 2008 and 2010 on a $0.5^\circ \times 0.5^\circ$ grid. (Sindelarova, ACP 2014)

FTIR sites location



Data retrieved over 7 regions → emission sources, remote area, areas influenced by long-range transport + land and sea scenes

Seasonal variation is taken account: 5 first days of each month on 2009 are retrieved

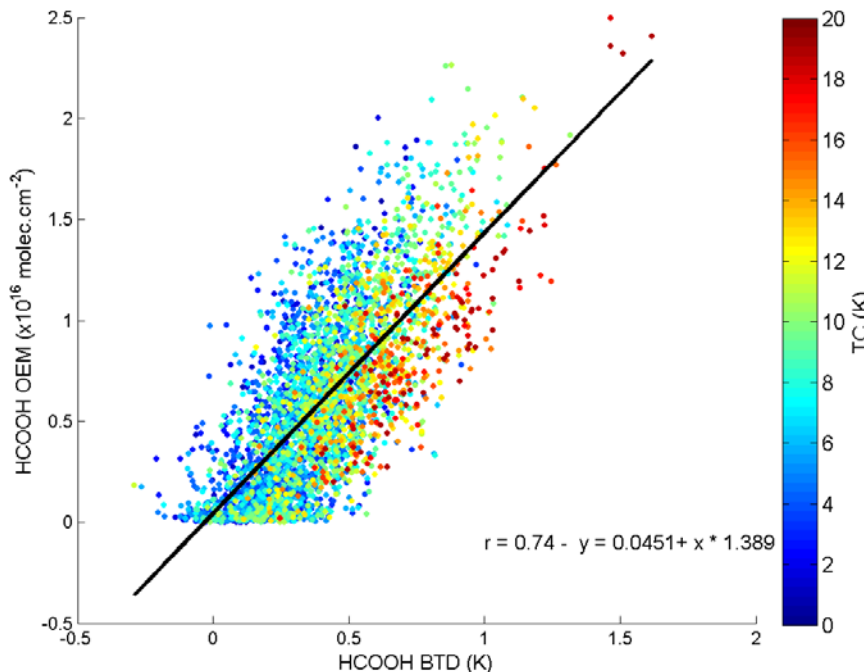
Region	Localization	Number of retrieved spectra
Africa N	6-7°N 18-22°E	265
Africa S	12-14°S 20-24°E	788
Amazonia	6-10°S 43-45°W	682
Atlantic	22-24°N 42-45°W	675
Australia	14-15°S 131-133°E	218
Pacific	20-22°S 140-142°E	472
Russia	50-54°N 60-62°E	538

HCOOH: Retrieval approach (2/2)



Parameters:

- 1095-1114 cm^{-1}
- Cloud fraction < 2%
- Same a priori than Razavi et al. (2011)
- Thermal contrast > 0 K ($T_{\text{surf}} - T_{\text{atm 1st layer}}$) (*Razavi et al. used TC > 5K*)
- day-time and night-time data used



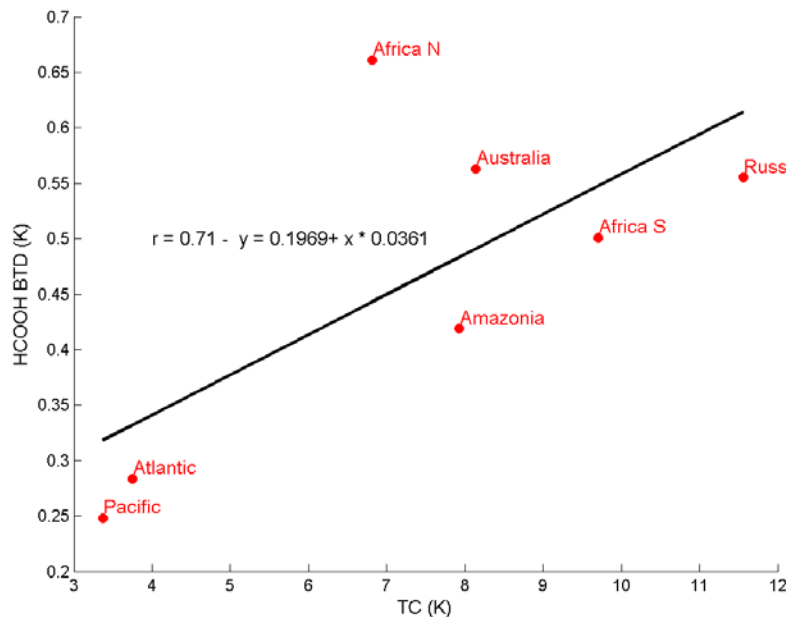
Good correlation between retrieved columns and ΔBT

But conversion is dependent on the TC

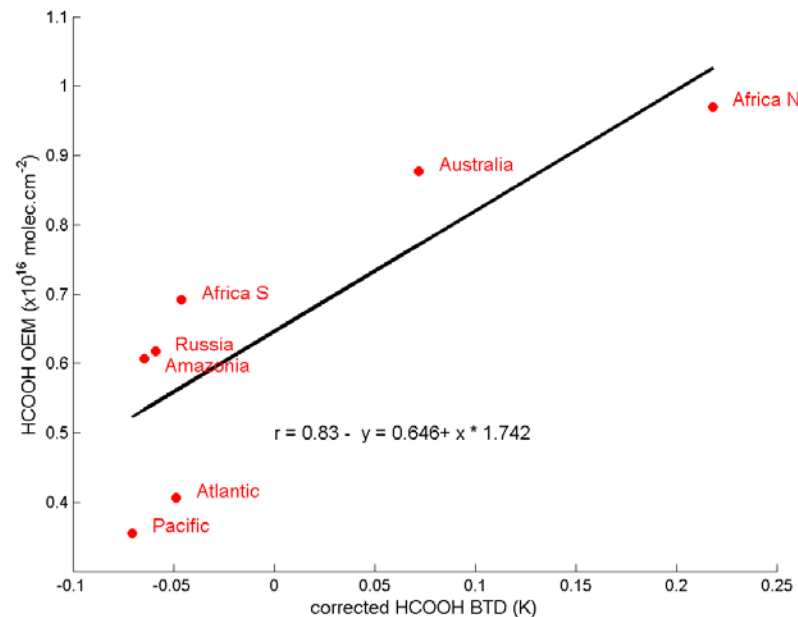
Establishment of a new dataset



Reduction of the thermal contrast dependence:
Mean over 7 regions



correlation between ΔBT and TC



correlation between retrieved columns and corrected ΔBT (TC)

Conversion using both relationships:

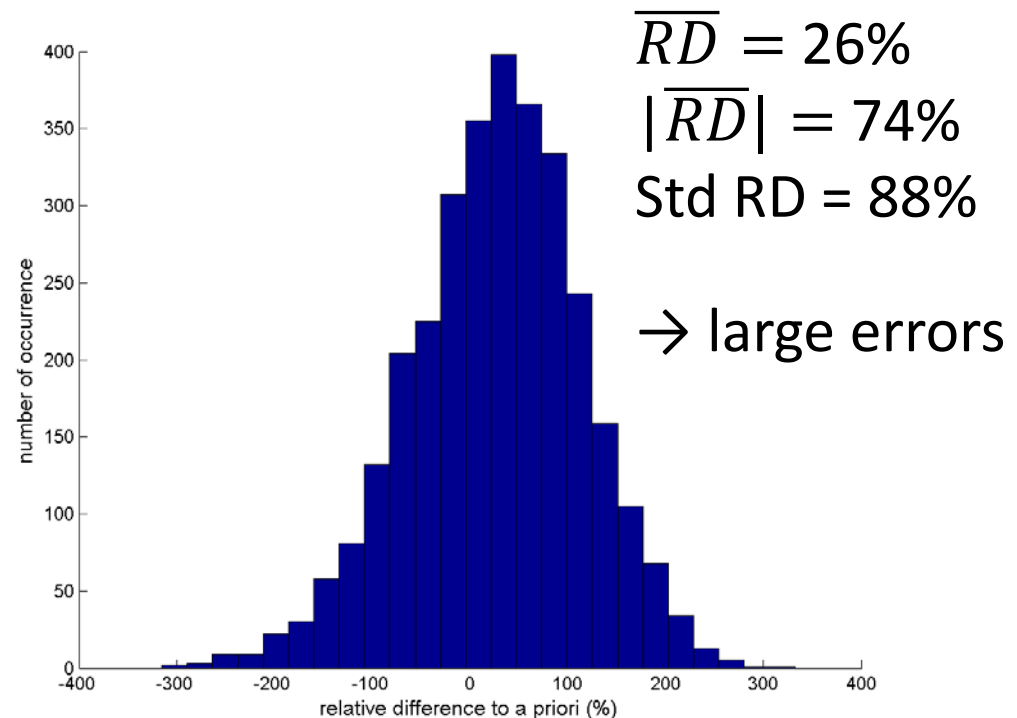
$$\text{Column} = 1.742 \times (\Delta BT - TC \times 0.0361 - 0.1969) + 0.646$$

3 terms:

- 1) the instrumental error
- 2) the error caused by the conversion between the ΔBT and the total column
- 3) the error from the retrievals.

total error by forward simulation (>3000 spectra):

- Gaussian distributed random noise ($\sigma = 0.15K$) added to the BT channels
- the conversion formula is applied on the calculated ΔBT .



Comparison with FTIR ($\pm 0.5^\circ$, daily mean)

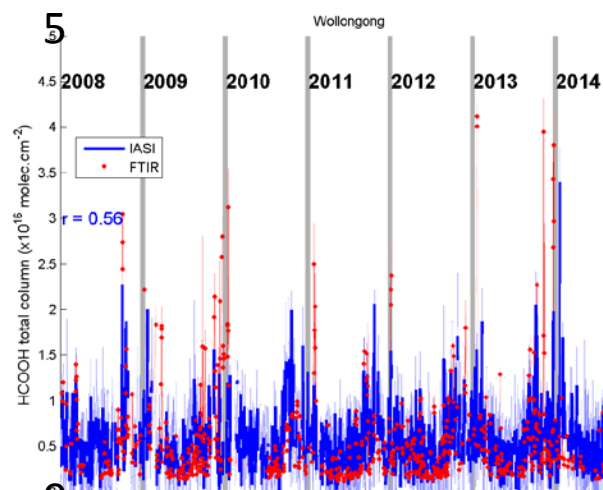
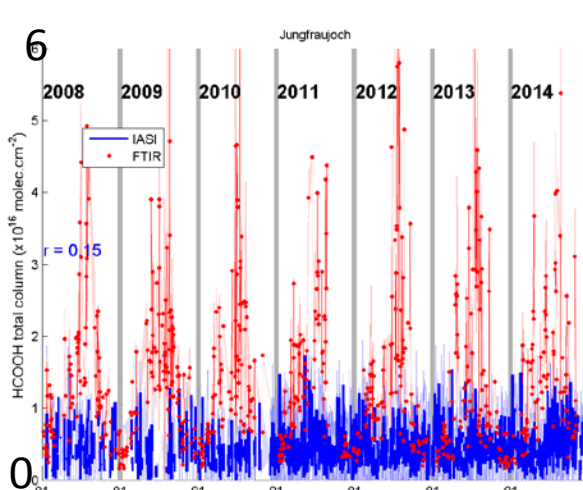


Simple altitude correction of total columns: $C' = C \times \exp(\text{Alt}/7.4)$

**Jungfraujoch
(3.6 km alt)**

R=0.15

Bias= 1.19×10^{16}
molec/cm²



**Wollongong (0
km alt)**

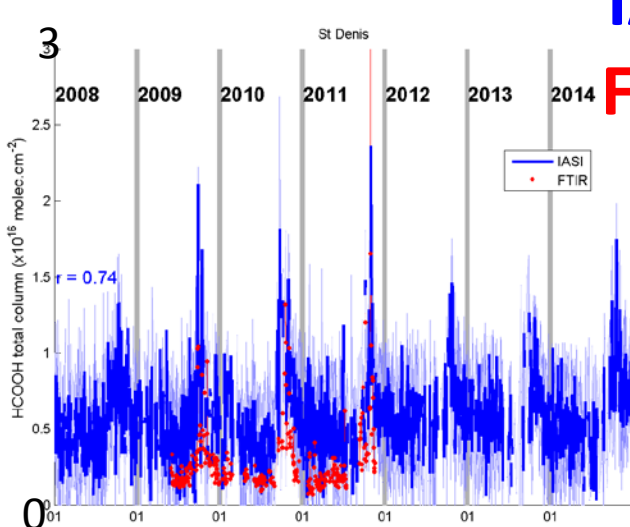
R=0.56

Bias= 0.01×10^{16}
molec/cm²

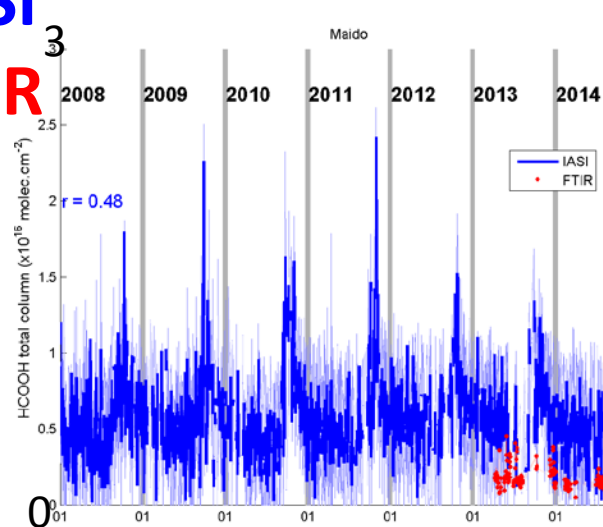
**Saint Denis
(La Réunion –
0.26 km alt)**

R=0.74

Bias= 0.30×10^{16}
molec/cm²



**IASI
FTIR**



**Maito
(La Réunion –
2.5 km alt)**

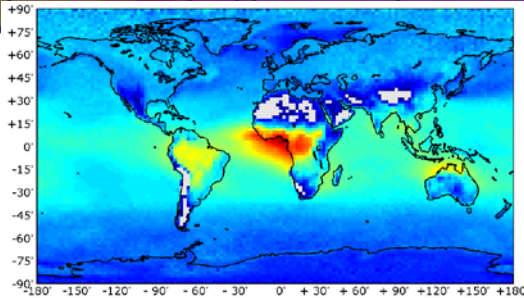
R=0.48

Bias= 0.32×10^{16}
molec/cm²

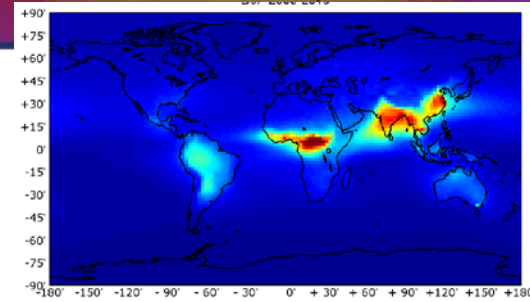
Seasonal Variation (global distribution)



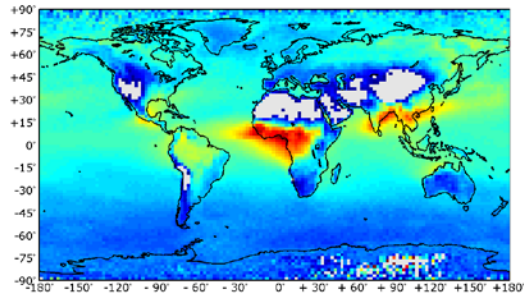
IASI
(gridded
IMAGESv2
=2°x2.5°)



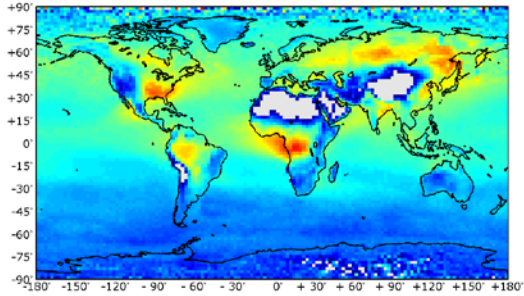
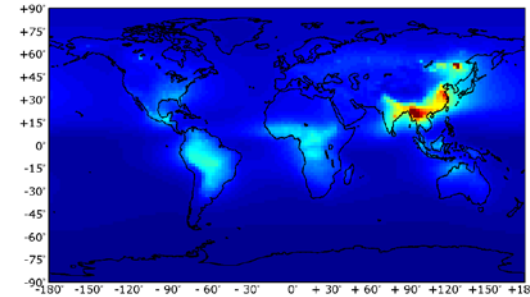
2008-2013
DJF



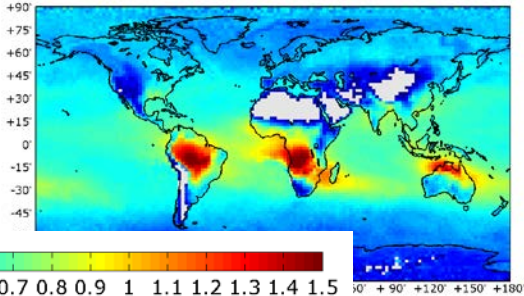
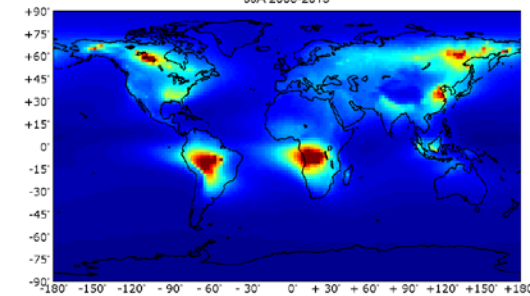
IMAGESv2



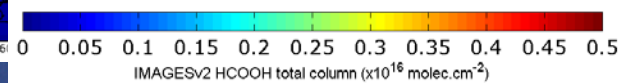
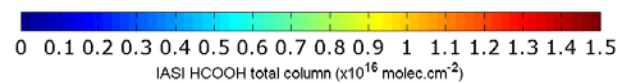
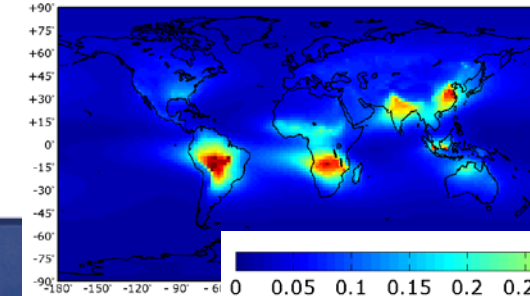
MAM

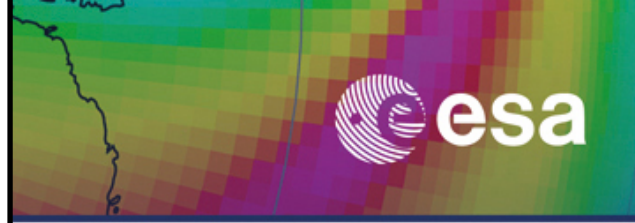
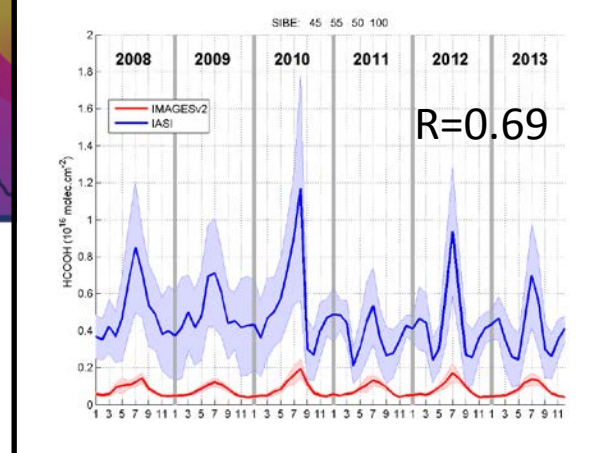
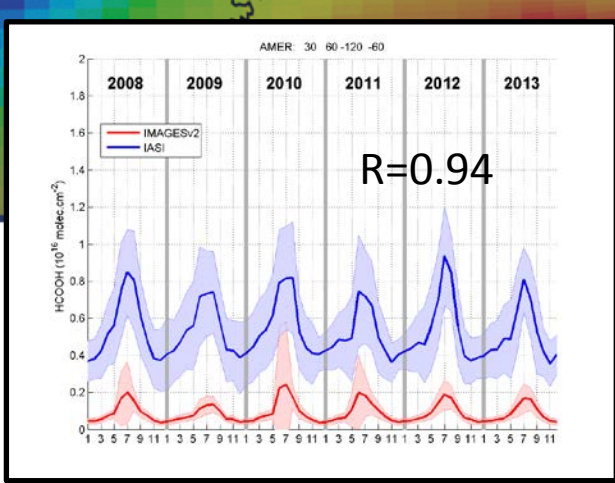


JJA

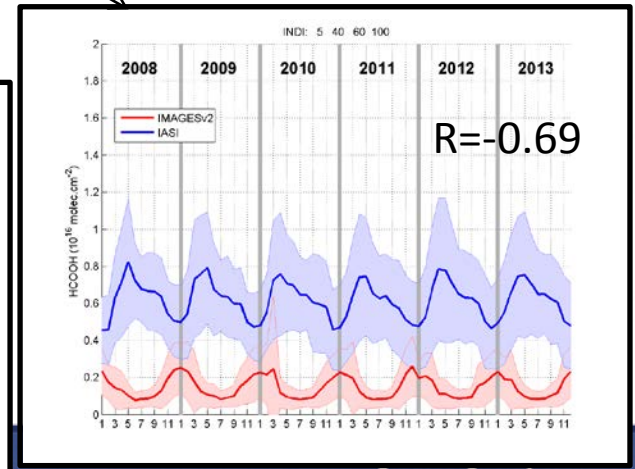
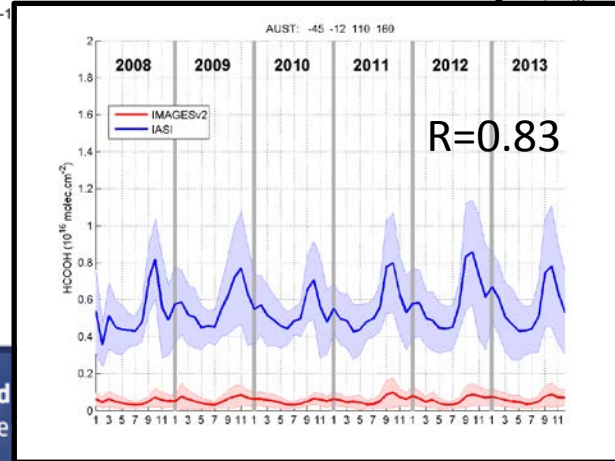
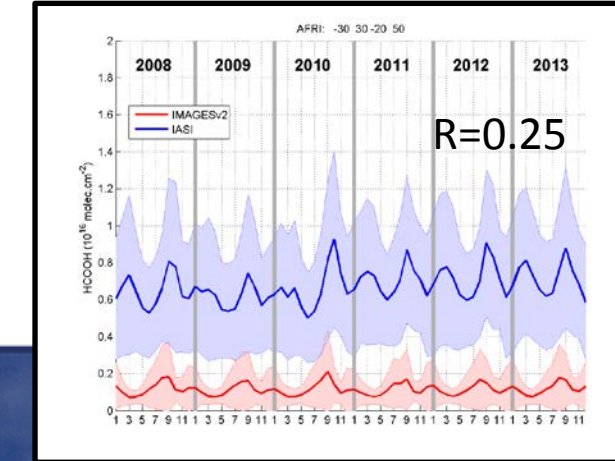
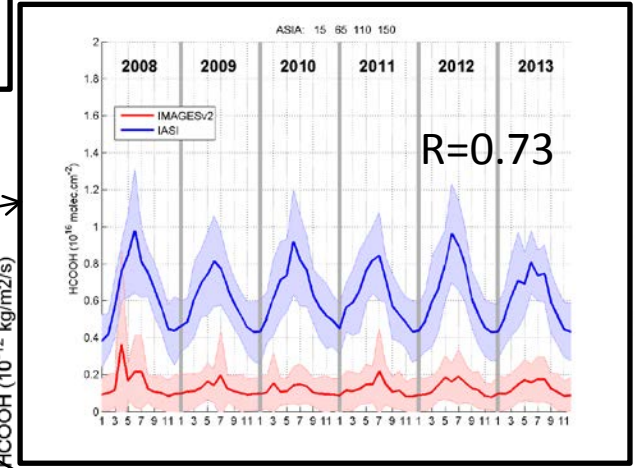
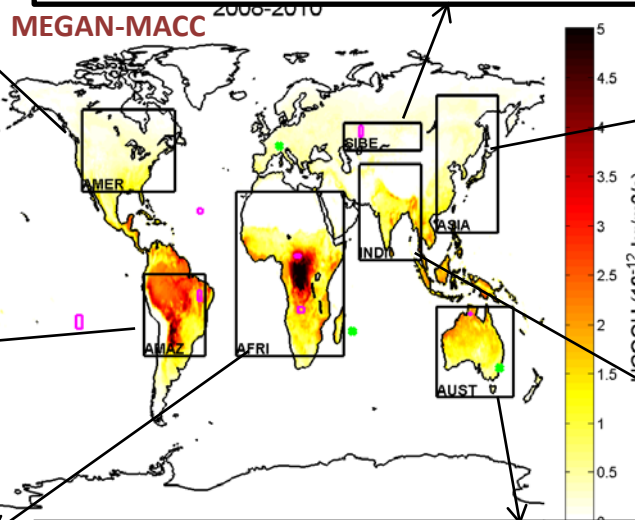
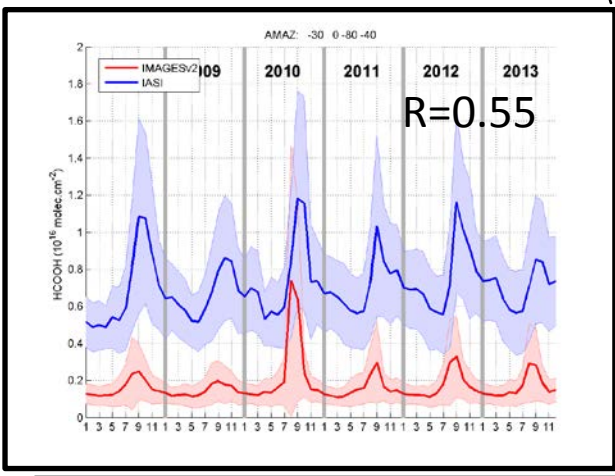


SON





IASI
IMAGESv2



- Global overview of HCOOH
- 7 years of data to analyze
- Detection hotspots (MiddleEast US, Asia...) & seasonal cycle



- No averaging kernels → difficulties to compare IASI total columns to FTIR and simulations

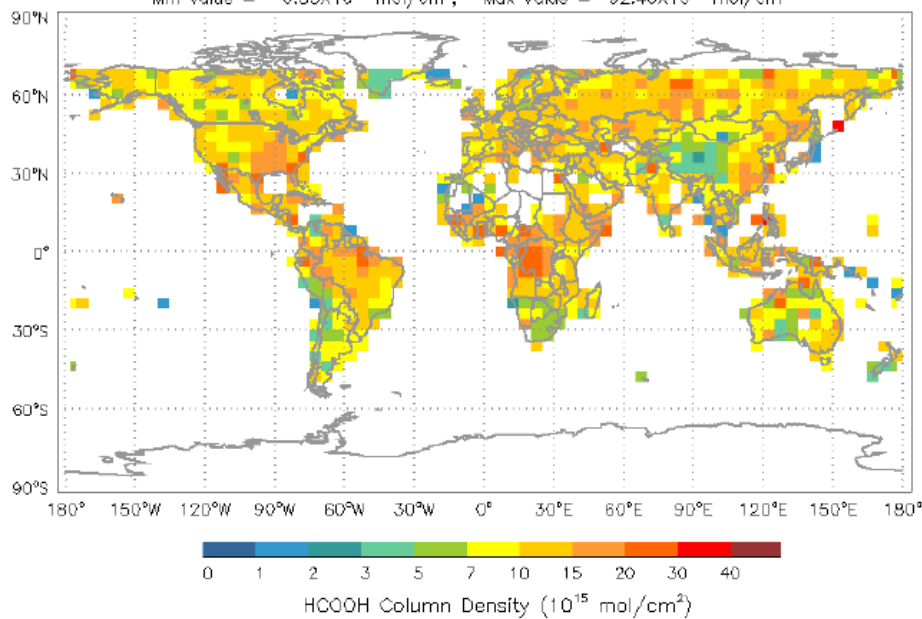


- Challenge in the interpretation of the data → misrepresentation of sources



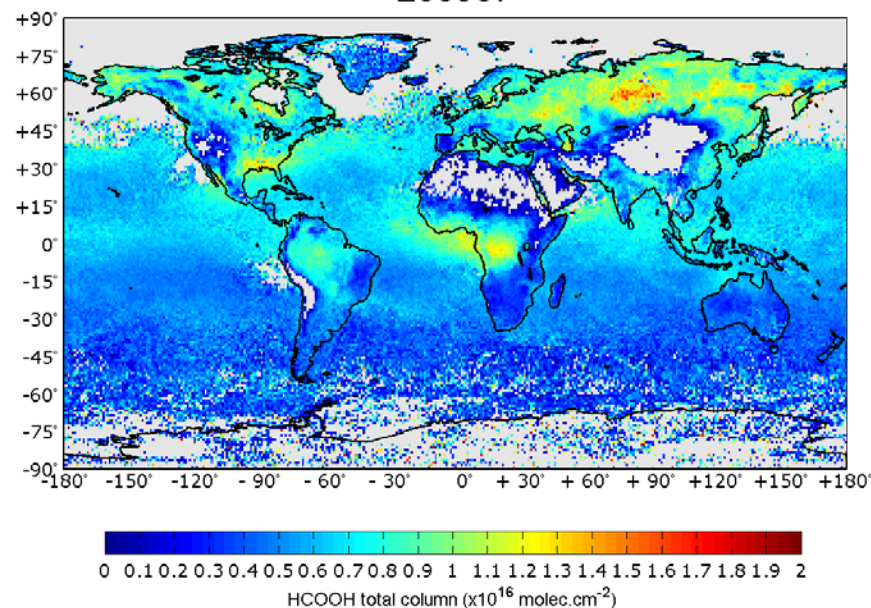
Extra slides

TES Level3 Image: HCOOH, 2009-07, Total Col Density (10^{15} mol/cm²)
 Min Value = 0.88×10^{15} mol/cm², Max Value = 92.40×10^{15} mol/cm²



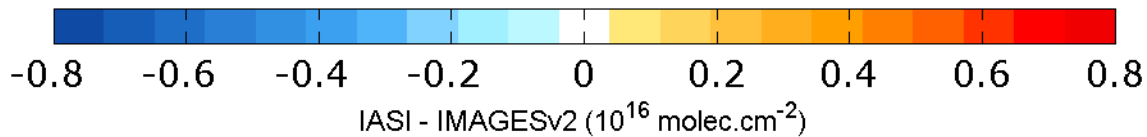
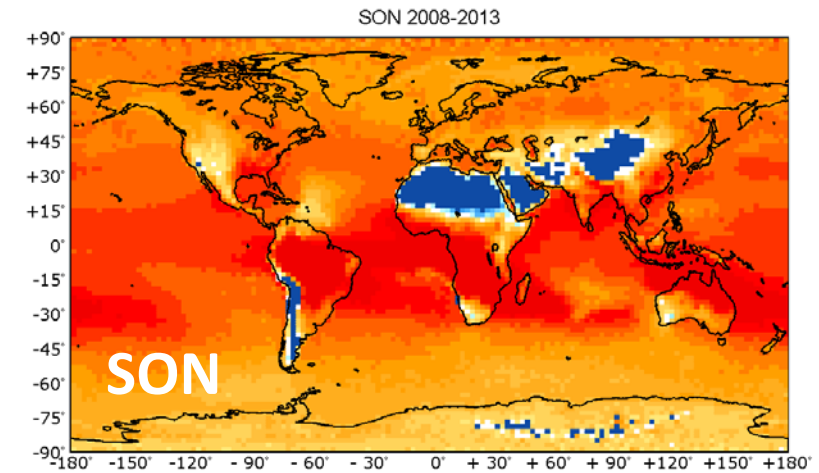
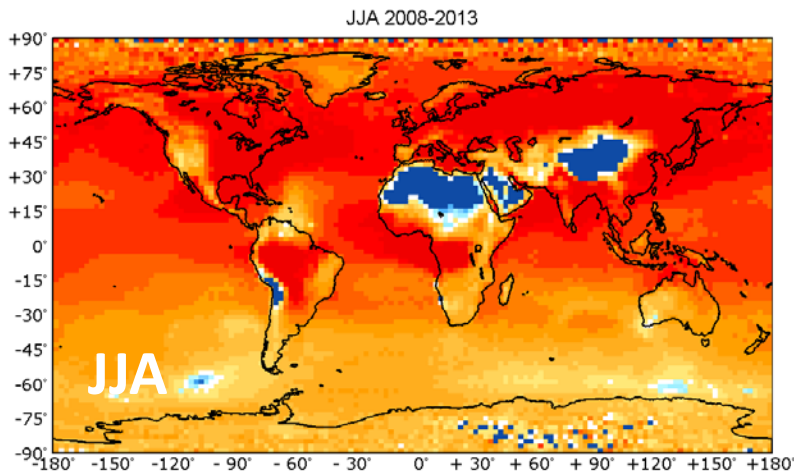
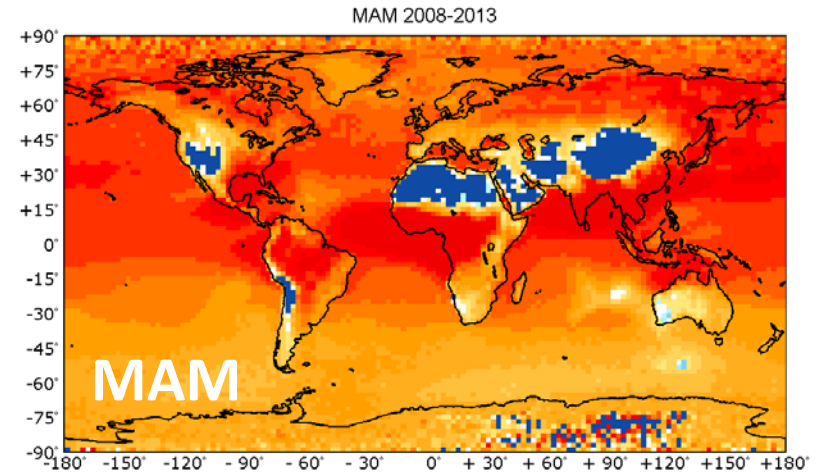
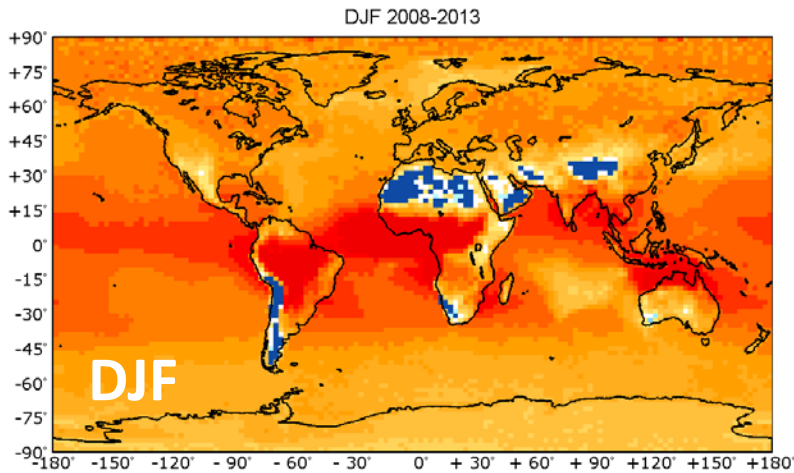
TES
 Cady-Pereira et al. AMT 2014

200907



IASI

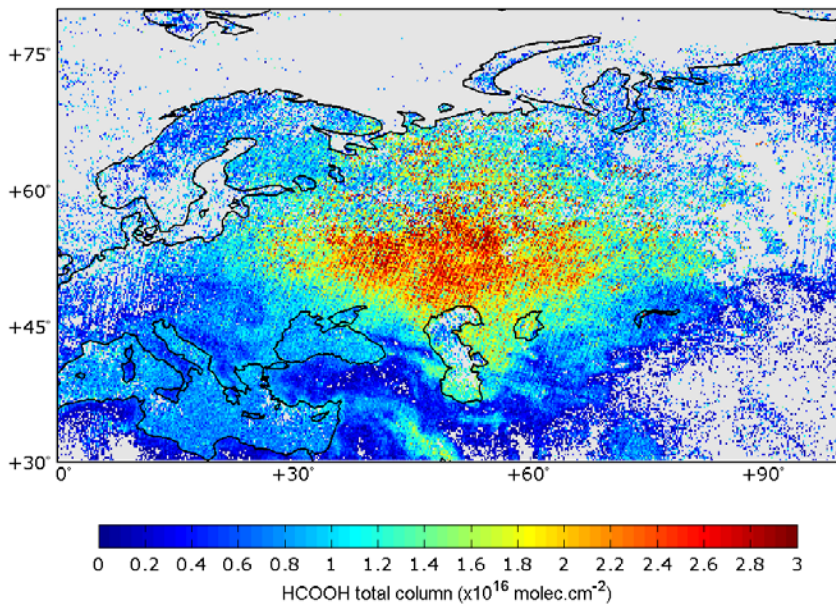
Seasonal Variation (global distribution)



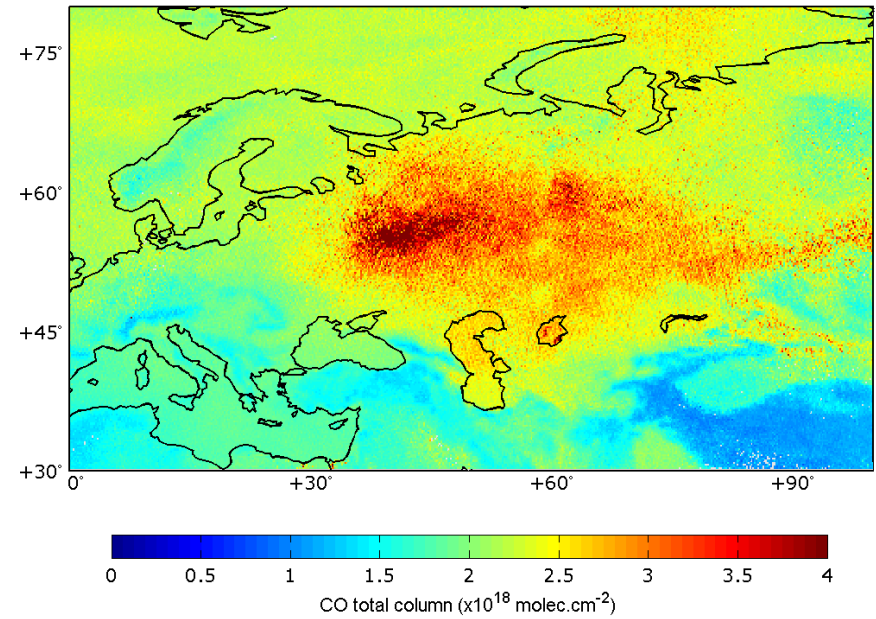
Detection of extreme events: fires over Russia



0.2°×0.2° 27 July – 27 August 2010 over Russia



HCOOH total column

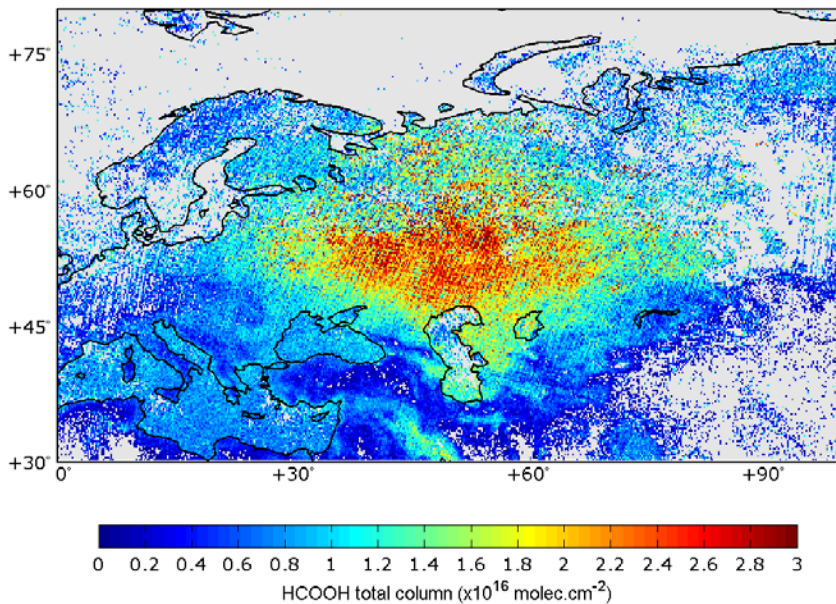


CO total column

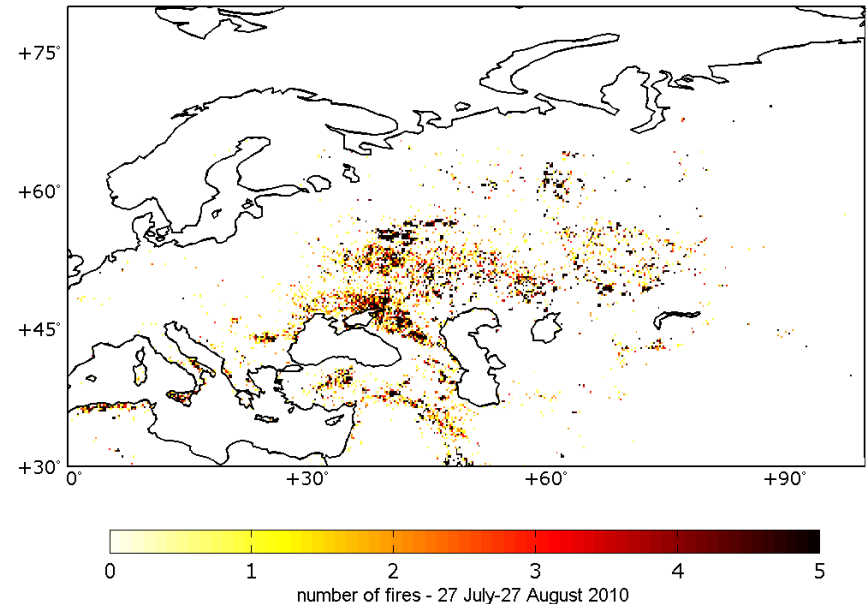
Detection of extreme events: fires over Russia



0.2°×0.2° 27 July – 27 August 2010 over Russia



HCOOH total column



MODIS hotspot